JOURNAL OF APPLIED ELECTROCHEMISTRY 24 (1994) 489–494

Polymer electrolyte-type electrochemical ozone generator with an oxygen cathode

M. KATOH, Y. NISHIKI, S. NAKAMATSU

Research and Development Division, Permelec Electrode Ltd, 1159 Ishikawa, Fujisawa-shi, Kanagawa 252, Japan

Received 23 August 1993; revised 30 November 1993

A new electrochemical ozone generator which has a proton exchange polymer membrane as an electrolyte, pure water as a source material and an oxygen diffusion electrode as a cathode was proposed to eliminate hydrogen evolution on the cathode and also to reduce electrolytic power consumption. The device was evaluated under varied operating conditions changing current density, temperature and oxygen flow rate. The water permeable high performance gas electrode enabled current density operation over 1.0 A cm^{-2} without generating hydrogen gas in the cathode side outlet gas. The power consumption was successfully reduced to two thirds of that of the hydrogen evolution type electrolyzer over a period of three months' operation.

List of symbols

- J_v flux of water vapour from the cathode chamber, $p_w \alpha i/4F$ (mol s^{-1} cm^{-2})
- J_l flux of liquid water from the cathode chamber (mol s^{-1} cm^{-2})
- J_d dragged water by proton transfer, miF (mol s^{-1} cm^{-2})
- J_e cathodically generated water, $i/2F$ (mol s^{-1} cm^{-2})
- p_w pressure ratio (saturated vapour pressure of water/total pressure)
- i current density for oxygen reduction (A cm^{-2})
- m number of water molecules dragged per proton (about 2.5 for Nafion® 117)
- F Faraday constant (96 487 C mol^{-1})
- α excess feed ratio = (oxygen feed rate/theoretical oxygen demand − 1)

1. Introduction

Demand for ozone has been progressively increasing in various fields such as treatment of drinking and waste water, industrial oxidation processes for chemicals and semiconductors, disinfection and therapy. Ozone is a strong oxidant which causes no secondary pollution problem. Silent discharge type ozone generators are in commercial use, but it is significant that contamination of metal particles coming from the discharge electrode material as well as NO_x, when air is used as an oxygen source, is harmful in some applications.

Stucki *et al.* [1] have recently developed an electrochemical ozone generator, wherein pure water is electrolyzed to produce hydrogen on the cathode and a mixture of ozone and oxygen on the anode. The anode and the cathode are pressed firmly onto a solid polymer electrolyte as a proton conductor and a gas separator. This electrolyser can generate highly concentrated and pure ozone. So, it enabled us to develop some new applications of ozone.

However, an electrochemical ozone generator has a large power consumption: $60 \sim 80$ Wh $(g\,O_3)^{-1}$, which is two to three times larger than that of the silent discharge type. Moreover, hydrogen gas generated on the cathode must be decomposed or treated safely if it is not useful at the production point.

Foller *et al.* [2] have proposed another type of ozone generator, wherein ozone gas is generated in an electrolyte containing fluoro anion, and the oxygen cathode is also applicable in this electrolytic system. It is surprising that the ozone concentration surpasses 35%. However, it is necessary to cool the electrolyte to produce such concentrated ozone. So, the overall power consumption might be almost the same as that of the pure water electrolysis type.

Based on the above developments, it is reasonable to consider utilizing an oxygen cathode in the pure water electrolytic system. This proposed new system reduces the cell voltage and power consumption and also eliminates hydrogen evolution on the cathode. Although the same kind of proposal has been made in a Japanese patent [3], it is said that the current density is rather low because the performance of the gas diffusion electrode is limited.

Gas diffusion electrodes with high performance are now available [4, 5], and work on operational parameters such as water mass balance [6, 7], temperature [8] and pressure [9] has been published. Thus, the use of such oxygen cathodes in electrolytic ozone generation is feasible.

A small scale and a pilot scale pure water electrolyser for ozone generation with an oxygen cathode were assembled. Performance parameters such as cell voltages, electrode potentials, current efficiencies for ozone and the possibility of hydrogen evolution

0021-891X

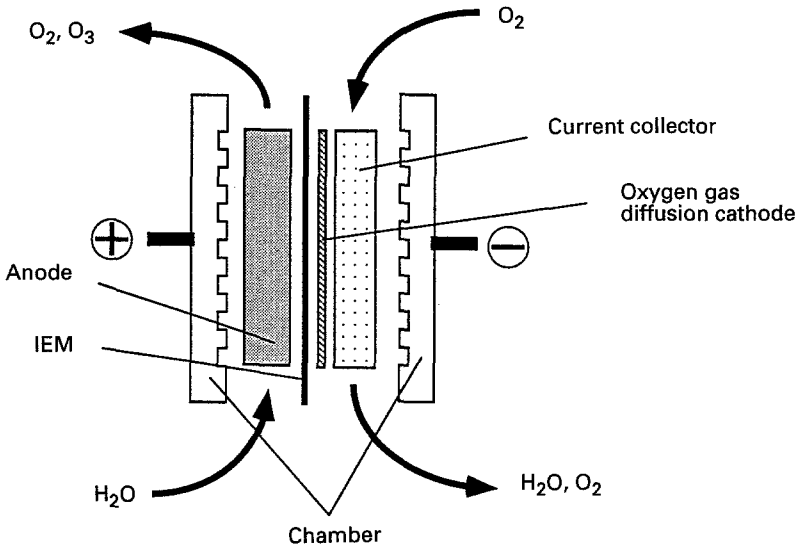

Fig. 1. Schematic drawing of electrochemical ozone generator with an oxygen diffusion cathode.

on the cathode were evaluated. The water balance and the results of durability tests of these electrolysers were also discussed.

2. Experimental details

A sintered porous titanium plate (Tokyo Rope Mfg) made of titanium fiber (60 μm diam., and 3 mm length) was used as an anode substrate. It was soaked and rinsed in 20 wt % hydrochloric acid at 60° C for 5 min, then the aqueous solution containing chloroplatinic acid was brush coated and baked at 500° C in air to form a platinum under layer coating by thermal decomposition. Lead dioxide was electrodeposited by two consecutive steps: α-PbO_2 was first anodically plated in an alkaline bath containing Pb^{2+} at 40° C and then β-PbO_2 was anodically deposited in an acidic saturated $Pb(NO_3)_2$ bath at 65° C. This procedure improves the adhesive strength between the lead dioxide and the titanium substrate [10]. The thickness of the PbO_2 layer was about 100 μm.

A Nafion® 117 membrane (Du Pont) was used as solid polymer electrolyte. This was pretreated in acid to convert the counter ions in the membrane to protons.

A plain carbon woven cloth (Zoltek, PWB-3) was used as cathode substrate. Carbon powder (Cabot Corporation, Vulcan XC-72) and PTFE powder (Du Pont Mitsui Fluorochemical, Co., 30J) was mixed and stirred in a beaker together with solvent naphtha and isopropyl alcohol. The mixture was loaded on both sides of the carbon cloth, and then baked at 350° C in air for 5 min to make a gas permeable conductive matrix. Allyl alcohol containing platinum salt was coated on one side and then baked at 350° C in air for 10 min. This catalyst loading method localized the electrocatalyst near the surface of the gas diffusion electrode facing the solid polymer electrolyte. The loaded amount of Pt was 5 $g\,m^{-2}$. Liquid Nafion® (Solution Technology, Inc.) was coated on the electrode in order to extend the reaction sites.

A woven mesh made of SUS316L was used as a cathode current collector and a gas zone. The cathode chamber was made of SUS316L and the anode chamber was made of titanium. Gaskets, fittings and tubes were all made of PTFE.

These components were assembled as shown in Fig. 1. A schematic flow diagram is illustrated in Fig. 2. Three types of cells, whose effective electrolytic areas were 5 cm^2 for potential measurement, 56 cm^2 and 300 cm^2 for electrolytic performance and durability test, were operated.

Deionized water was fed into the anode chamber using a metering pump, and the anolyte was self-circulated by the gas life effect. Oxygen gas (99.999%) was supplied to the cathode chamber from a gas cylinder for temporary operation and a PSA oxygen generator (Taiyo Sanso Ltd, OX–4, $O_2 > 90\%$) was used for a long term operation. The oxygen feed rate was varied in the range 1 to 10 times larger than the theoretical consumption for each current load. Argon gas was fed to the cathode chamber when hydrogen evolution occurred on the cathode. The cell temperature was controlled at 20 to 50° C by an internal heat exchanger built in the anode side gas–liquid separator. Most of the experiments were carried out at 30° C because the ozone current efficiency has a maximum value at 30° C as shown in Fig. 3. All the experiments were carried out under atmospheric pressure.

Cathode potentials were measured against Hg/Hg_2SO_4 reference electrode using the current interruption method. The reference electrode was immersed in 0.5 M sulphuric acid solution in which the edge of the Nafion® 117 membrane was also immersed. A current interrupter (Hokuto Denko Corp.) and a digital oscilloscope (Iwatsu Corp., DMS6440) were employed for this measurement. Ozone current efficiencies were measured by iodometry. Hydrogen gas in the oxygen cathode exit gas was analysed by gas chromatograph (Hitachi Ltd,

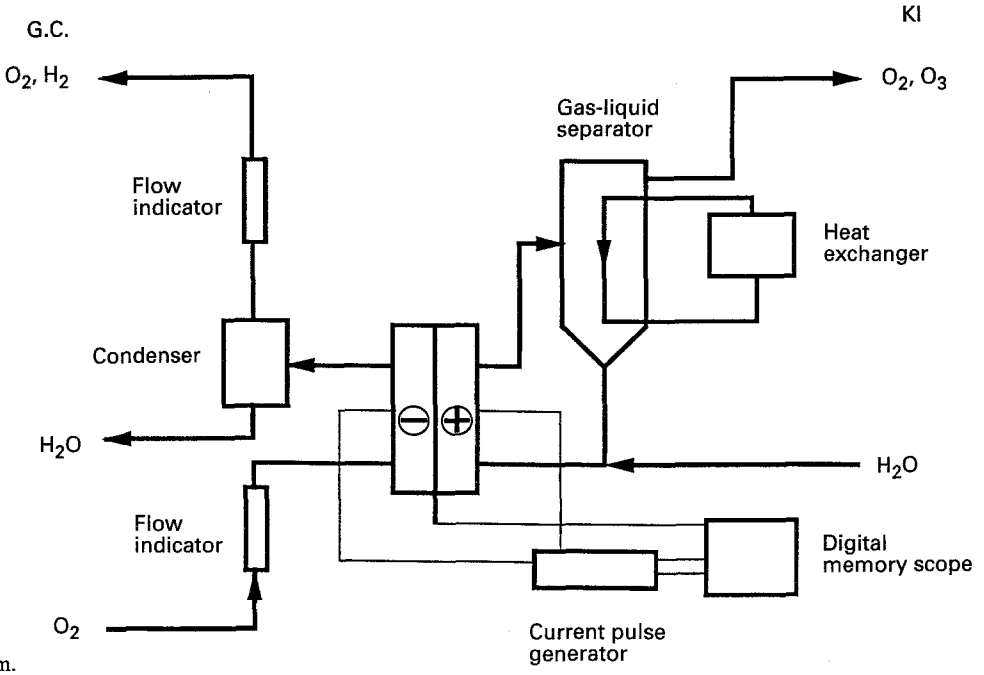

Fig. 2. Schematic flow diagram.

G-5000) using 99.999% helium as carrier gas. This method detects hydrogen below 1 p.p.m.

3. Results and discussion

The electrode reactions and their standard potentials are as follows:
Anode reactions:

$$H_2O = O_2 + 4H^+ + 4e^- \quad E_0 = 1.23\,V \quad (1)$$

$$H_2O = O_3 + 6H^+ + 6e^- \quad E_0 = 1.51\,V \quad (2)$$

$$O_2 + H_2O = O_3 + 2H^+ + 2e^- \quad E_0 = 2.07\,V \quad (3)$$

Cathode reaction:

$$O_2 + 4H^+ + 4e^- = 2H_2O \quad E_0 = 1.23\,V \quad (4)$$

$$2H^+ + 2e^- = H_2 \quad E_0 = 0.00\,V \quad (5)$$

Considering the potential difference between two anodic competing Reactions 1 and 2, ozone generation is strongly dependent on the anode catalyst and reaction kinetic scheme. β-PbO_2 has very high oxygen evolution overpotential and is suitable for ozone generation.

By changing the cathode reaction from hydrogen evolution (5) to oxygen reduction (4), the cell voltage is reduced by 1.23 V. An example of the difference in cell voltage between the hydrogen evolution and oxygen reduction approaches to water electrolysis is shown in Fig. 4. At 1 A cm^{-2}, the cell voltage with oxygen reduction is 0.85 V lower than that with hydrogen evolution. The cathode potentials are plotted at several oxygen partial pressures in Fig. 5 compared to the hydrogen evolution electrode. Here the oxygen content was adjusted by adding argon to oxygen gas. The potentials strongly depend on the oxygen partial pressure at high current densities. Hydrogen was not detected in the cathode outlet oxygen gas up to 2 A cm^{-2}, which means that the cathode potential did not reach the hydrogen evolution

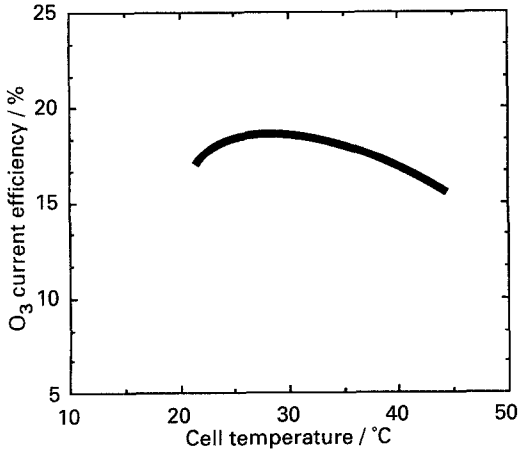

Fig. 3. Dependence of ozone current efficiency on temperature in hydrogen evolution type electrolyser. Current density 1.0 A cm^{-2}; electrode area 56 cm^2.

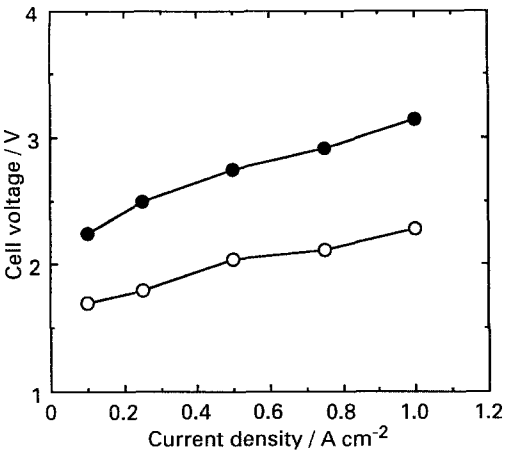

Fig. 4. Dependence of cell voltage on current density. (●—●) without oxygen feed; (○—○) with oxygen feed. Feed rate 16.7 cm^3 s^{-1}; electrolyte area 56 cm^2; anolyte temp. 30° C.

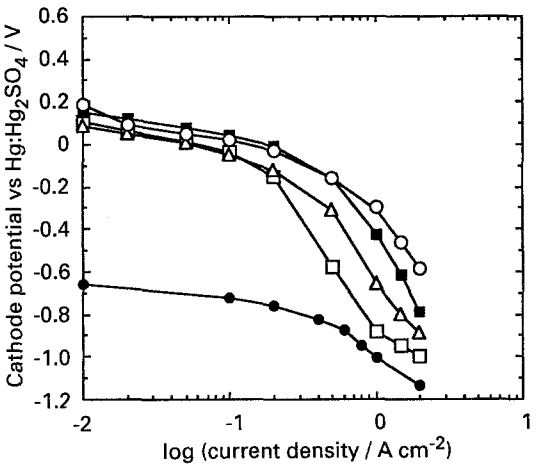

Fig. 5. Cathodic polarization curves under various oxygen pressures: (□) 0.2, (△) 0.5, (■) 0.8, (○) 1.0 and (●) Ar feed. Electrode area 5 cm^2; anolyte temp. 30° C; oxygen feed 16.7 $cm3\ s^{-1}$.

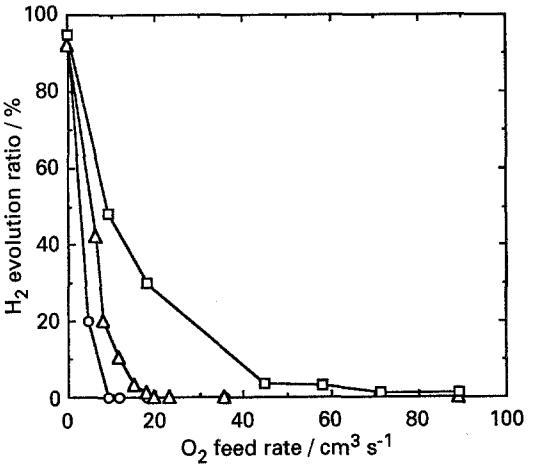

Fig. 7. Dependence of hydrogen evolution ratio on oxygen feed rate. Current densities: (○—○) 0.5, (△—△) 1.1, (□—□) 1.5 A cm^{-2}. Electrode area 300 cm^2; anolyte temp. 30° C.

potential. The potential difference between the two reactions was 0.70 V at 1 A cm^{-2}.

Comparing these two difference values, it is curious that the difference between the cell voltages is 0.15 V larger than that of the cathode potentials. The overpotential of the oxygen cathode was found to be 0.90 V at 1 A cm^{-2}, while the overpotential of the hydrogen cathode was about 0.35 V. These overpotentials result in heat and raise the temperature at the cathodes, which leads to reduction of the ohmic drop of the membrane, especially in the case of the oxygen cathode. This is a possible explanation of the difference of 0.15 V.

The dependence of cell voltage on the oxygen feed rate is shown in Fig. 6. When the oxygen flow rate was increased, the cell voltage gradually decreased and reached an almost constant value depending on current load. When the flow rate was smaller than the theoretical one, the cell voltage reflected the mixed potential of Reactions 4 and 5. The dependence of the hydrogen evolution ratio on the oxygen flow rate is also shown in Fig. 7. This suggests that oxygen must be fed in excess to depress the hydrogen evolution reaction on the cathode and that the excess oxygen ratio, α, need not exceed 0.2 below

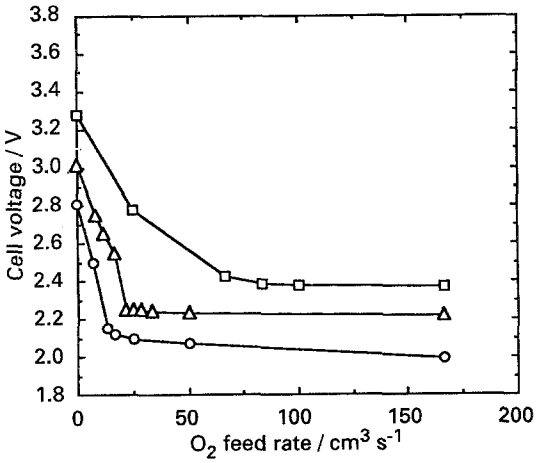

Fig. 6. Dependence of cell voltage on oxygen feed rate. Current densities: (○—○) 0.5, (△—△) 1.1, (□—□) 1.5 A cm^{-2}. Electrode area 300 cm^2; anolyte temp. 30° C.

1.1 A cm^{-2} although α should be larger than 4 at 1.5 A cm^{-2}.

This result means that no water flooding inside the cathode occurred even in the case of a low oxygen flow rate. The electrolyser must be operated at ambient temperature to maintain high ozone current efficiency, although polymer electrolyte fuel cells are normally operated at temperatures higher than 80° C. Thus, most of the water coming from the anode side to the cathode side is not vapour but liquid. This is one reason why a liquid permeable gas diffusion electrode is successful.

The advantage of a liquid water permeable gas electrode was confirmed by calculating the water mass balance at the oxygen cathode. Suppose that J_v is the flux of water vapour from the cathode chamber (mol s^{-1} cm^{-2}), that J_l is the flux of liquid water from the cathode chamber as water droplets, that J_d is dragged water by proton transfer and that J_e is water generated on the cathode according to Equation 4, the following relation exists between these parameters during steady state electrolysis. The schematic diagram for the water balance is shown in Fig. 8.

$$J_v + J_l = J_d + J_e \quad (6)$$

The water flux caused by diffusion has to be considered in Equation 6 if there is a large vapour pressure difference between the sides of the membrane. However, this can be neglected here. J_l depends strongly on the characteristics and structure of the cathode, and the gas diffusion electrode should be designed so that $J_v + J_l$ is larger than $J_d + J_e$.

Fujita *et al.* [11] have previously proposed an equation relating to their electrolytic system having an oxygen evolution anode and an oxygen reduction cathode in a polymer electrolyte electrolyser. According to their study, limiting current density can be calculated as 0.013 A cm^{-2} at 40° C even when α is 1.0. This value is one eighteenth of the present experimental result; 1.1 A cm^{-2}. This fact indicates that the main route for water transfer is J_l; water transfer as liquid. Therefore, it is important to consider, not only hydro-

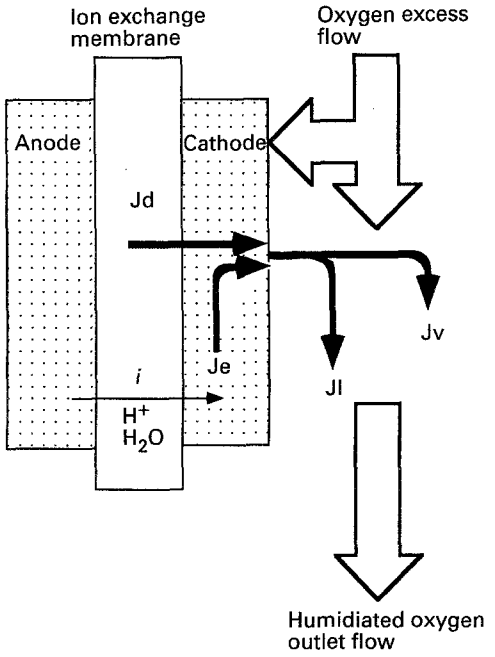

Fig. 8. Schematic diagram for water balance.

phobicity, but also water permeability relating to pore size and distribution of the gas electrode in order to obtain good performance.

The critical operational condition relating to current density and anolyte temperature is shown in Fig. 9, which was determined by the cell voltages and hydrogen content in the cathode outlet gas. In this test the cell voltage increased with temperature, which is abnormal for an ordinary electrolytic cell. The result shown in Fig. 5 suggests that the oxygen reduction reaction is controlled by mass transfer at very high current densities. This abnormal temperature effect can be explained as follows; the water vapour pressure in the cathode chamber increases when the anolyte temperature increases which leads to low oxygen partial pressure at the cathode resulting in higher cathode overpotential, and causing hydrogen evolution and higher cell voltage. Therefore, the anolyte must be kept at ambient temperature both for high ozone current efficiency and for safe operation of the oxygen cathode.

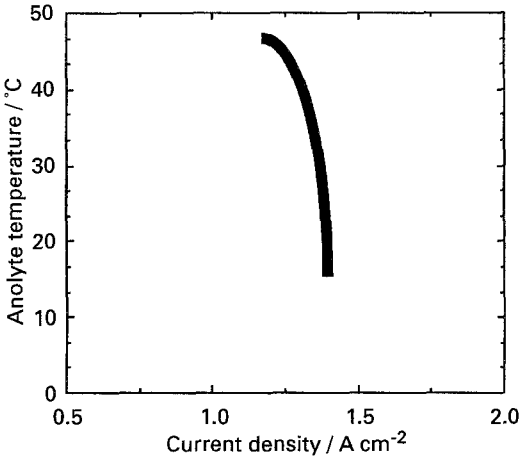

Fig. 9. Critical operational conditions relating to current density and temperature (left side of the solid curve corresponds to the safe region without generating hydrogen). Electrode area is 56 cm^2; oxygen feed rate 10 cm^3 s^{-1}.

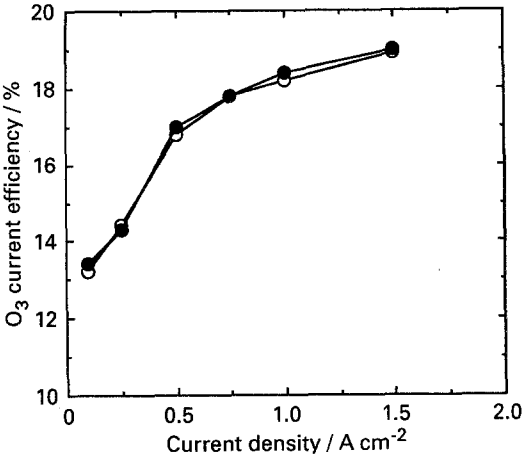

Fig. 10. Dependence of ozone current efficiency on current density. (●—●) Without oxygen feed; (○—○) with oxygen feed). Feed rate 16.7 cm^3 s^{-1}; electrode area 56 cm^2; anolyte temp. 30° C.

The relation between ozone current efficiency and current density is shown in Fig. 10. Current efficiency increased with current density, and 13% to 19% ozone was obtained at 1 to 1.5 A cm^{-2}. Little difference was found between the hydrogen evolution type and the oxygen reduction type. This suggests that the local heat generated at the cathode surface does not have much effect on the anode surface, at least as far as the current efficiency is concerned. A computational approach is required for a more quantitive estimate of heat fluxes and temperatures within the cell. Results of durability tests at 1 A cm^{-2} and 30° C are shown in Figs 11 and 12. The cell voltage of the oxygen cathode type ozone generator was stable at 2.20 ~ 2.35 V and the current efficiency was 15% ~ 17%. No hydrogen was detected in the outlet gas from the cathode chamber. Comparison of power consumption is shown in Table 1. The power consumption of the oxygen cathode type was 40 ~ 50 Wh (g O_3)$^{-1}$, which is two-thirds of that of the hydrogen evolution type, although an additional power consumption should be considered in the case of using a PSA oxygen generator.

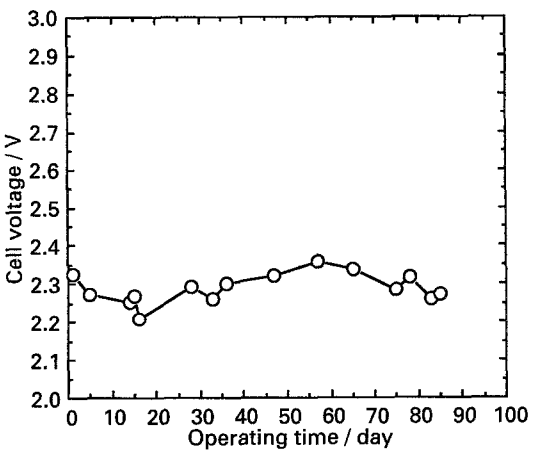

Fig. 11. Stability of cell voltage in durability test. Current density 1.0 A cm^{-2}; anolyte temp. 30° C; oxygen feed rate 16.7 cm^3 s^{-1}; electrode area 56 cm^2.

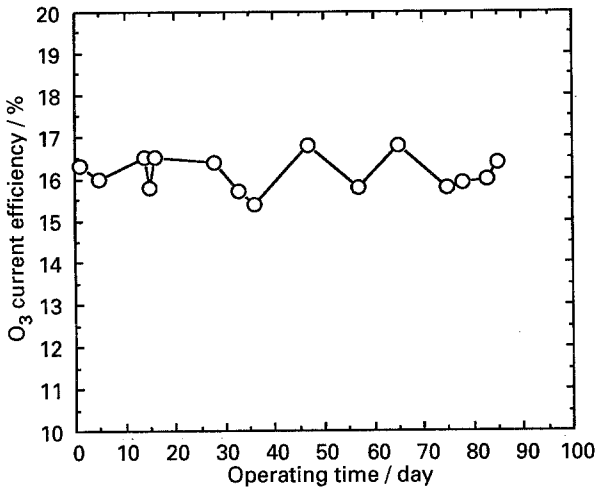

Fig. 12. Stability of ozone current efficiency in durability test. Current density 1.0 A cm^{-2}; anolyte temp. 30° C; oxygen feed rate 16.7 cm^3 s^{-1}; electrode area 56 cm^2.

4. Conclusions

A new type of electrochemical ozone generator having a high performance gas diffusion electrode as an oxygen cathode was developed and the following performances were obtained.

(i) The electrolyser could be operated safely without hydrogen evolution at current densities higher than 1.0 A cm^{-2}.

(ii) The saving in power consumption was more than 30% compared to the hydrogen evolution type electrochemical ozone generator.

(iii) Electrolytic performance such as cell voltage and ozone current efficiency was stable over three months.

(iv) Operating temperature must be controlled around 30° C in order to achieve good performance of the oxygen cathode and also to maintain good ozone current efficiency.

Table 1. Typical power consumption for different cathode reaction

Cathode reaction	*Cell voltage* /V	*O_3 current efficiency* /%	*Power consumption* /Wh $(g\,O_3)^{-1}$
Hydrogen evolution	3.2–3.5	15–18	60–80
Oxygen reduction	2.1–2.3	15–18	40–50

Acknowledgement

The authors are grateful to S. Wakita and Miss I. Inoue for technical support, to Prof. G. Faita (De Nora Permelec S.p.A) for his helpful suggestions and M. Shimada (President of Permelec Electrode Ltd) for permission to publish this paper.

References

[1] S. Stucki, G. Theis, R. Kötz and H. J. Christen, *J. Electrochem. Soc.* **132** (1985) 367.
[2] P. C. Foller and M. L. Goodwin, 'Ozone: Science and Engineering', Pergamon Press, (Oxford) Vol 6, (1984) p. 29.
[3] *Japanese 'Laid-open' Patent H2-44 908.*
[4] E. A. Ticianelli, C. R. Derouin and S. Srinivasan, *J. Electroanal. Chem.* **251** (1988) 275.
[5] E. A. Ticianelli, C. R. Derouin, A. Redondo and S. Srinivasan, *J. Electrochem. Soc.* **135** (1988) 2210.
[6] D. M. Bernardi, *ibid.* **137** (1990) 3344.
[7] T. E. Springer, T. A. Zawodzinski and S. Gottesfeld, *ibid.* **138** (1991) 2334.
[8] A. Parthasarathy, S. Srinivasan and A. J. Appleby, *ibid.* **139** (1992) 2530.
[9] *Idem, ibid.* **139** (1992) 2856.
[10] *US Patent 4 822 459.*
[11] Y. Fujita and I. Tanigawa, *Denki Kagaku* **53** (1985) 812.